Applied Mathematical Modelling 38 (2014) 4396–4408

Contents lists available at ScienceDirect

Applied Mathematical Modelling

journal homepage: www.elsevier.com/locate/apm

An accurate application of the integral method applied to the diffusion of oxygen in absorbing tissue

S.L. Mitchell *

Mathematics Applications Consortium for Science and Industry (MACSI), Department of Mathematics and Statistics, University of Limerick, Limerick, Ireland

ARTICLE INFO

Article history:
Received 4 December 2012
Received in revised form 25 September 2013
Accepted 13 February 2014
Available online 28 February 2014

Keywords:
Oxygen diffusion
Moving boundary problem
Heat balance integral method

ABSTRACT

Accurate integral methods are applied to a one dimensional moving boundary problem describing the diffusion of oxygen in absorbing tissue. These methods have been well studied for classic Stefan problems but this situation is unusual because there is no condition which contains the velocity of the moving boundary explicitly. This paper begins by giving a short time solution and then discusses some of the previous integral methods found in the literature. The main drawbacks of these solutions are that they cannot be solved from $t = 0$ and also cannot determine the end behaviour. This is due to the non-uniform initial profile which integral methods typically fail to capture. The use of a novel transformation removes this non-uniformity and, on applying optimal integral methods to the resulting system, leads to simple and yet very accurate approximate solutions that overcome the deficiencies of previous methods.

1. Introduction

This paper investigates the one-dimensional problem of oxygen diffusion in a medium which simultaneously absorbs the oxygen, as originally posed by Crank and Gupta [1], and often called the *Crank and Gupta problem* in the literature. It is an unusual moving boundary problem because the conditions which determine the movement of the boundary are different to classic Stefan problems. The situation considered here has no Stefan condition which explicitly contains the velocity of the moving boundary; instead zero concentration and zero flux are prescribed there. This is an example of a non-linear parabolic moving boundary problem, without an exact solution, and so approximate or numerical solutions must be sought. By now there is an extensive literature on numerical solutions to the problem, see for example [2–9] and references therein. Mitchell and Vynnycky [9] have recently developed a numerical method which is formally second order accurate for all variables and considers in detail the actual value of the time, t_e, at which the oxygen is depleted. These issues had either not previously been resolved conclusively, or not considered at all. The method applies the Keller box finite difference scheme [10–12] to the boundary immobilised system and is the numerical solution used here to compare with the integral solutions.

Goodman [13–15] originally proposed using an *integral method* for solving thermal and Stefan problems, which was an adaptation of the Karman–Pohlhausen integral method [16] for analysing boundary layers; see [17] for a translated account of this work. In the context of heat conduction problems, it is known as the heat balance integral method (HBIM) and since exact solutions have been found for many problems in heat transfer, the HBIM has made its greatest impact on Stefan problems, where very few exact solutions exist. Despite the fact that HBIMs are not always as accurate as numerical solutions,

* Tel.: +353 61202259.
E-mail address: sarah.mitchell@ul.ie

http://dx.doi.org/10.1016/j.apm.2014.02.021
0307-904X/

they remains popular due to their simplicity and the fact that they produce analytic solutions for a wide range of problems and parameter values. More recently, Mitchell and Myers [18–27] have published a series of papers devoted to integral methods applied to a variety of thermal and moving boundary problems. A comprehensive review of the HBIM and its variants is given in [22], along with a discussion of its disadvantages. Mitchell and Myers have also investigated ways to improve the HBIM by using an unknown exponent in the approximating profile to describe the dependent variable (usually the temperature) [23–26], and these have always given more accurate solutions than the classic HBIM solutions.

Crank and Gupta [1] were the first to consider integral methods applied to the oxygen diffusion problem. They noted that *integral methods are not every amenable to cases of non-uniform initial distributions* and their solution reflected this. It was not valid for small times and also broke down before all the oxygen had been depleted. Gupta and Banik [28] discussed a variant of the Crank and Gupta profile but its results were similar in accuracy and also had the same drawbacks. Although integral methods have been applied to this problem more recently by Catal [4], these issues have still not been addressed and, in fact, their results are less accurate results than both the Crank and Gupta and Gupta and Banik profiles. Ahmed [2,3] has embedded an integral method into a numerical scheme by applying various moments of the integral formulation and creating a system of linear equations. However, the resulting algorithms are complicated and their accuracy is not clear. In this paper we use a novel transformation which removes the non-uniform initial distribution and inconsistencies at $(x, t) = (0, 0)$. A relatively simple integral method, based on the *combined integral method* (CIM) [23,26] can then be applied which yields very accurate approximate solutions and overcomes the deficiencies of previous work.

The layout of this paper is as follows. In Section 2 we give the governing non-dimensional equations for the oxygen diffusion problem. In Section 3 we discuss the short time solution and then move onto describing the Crank and Gupta and Gupta and Banik profiles in Section 4. We also investigate a simple transformation to remove the non-unform initial distribution; however this alone does not remove the inconsistencies at $(0, 0)$ and the resulting solutions are very inaccurate. In Section 5 we perform an analysis on the short time solution which guides us to a further transformation leading to a model which is consistent at $(0, 0)$. We then apply the CIM with three different profiles to this transformed system, comparing results with the aforementioned numerical solution [9], and examine the behaviour as $t \to t_e^-$. Finally, in Section 6 we draw conclusions.

2. Mathematical formulation

In non-dimensional form the system to describe the oxygen diffusion problem is given by

$$\frac{\partial u}{\partial t} = \frac{\partial^2 u}{\partial x^2} - 1, \quad 0 < x < s(t), \tag{1}$$

$$\frac{\partial u}{\partial x} = 0, \quad \text{at} \quad x = 0, \tag{2}$$

$$u = \frac{\partial u}{\partial x} = 0, \quad \text{at} \quad x = s, \tag{3}$$

$$u = \frac{1}{2}(1 - x)^2, \quad 0 \leqslant x \leqslant 1, \quad \text{at} \quad t = 0, \tag{4}$$

with $s(0) = 1$.

We can obtain an expression for the location of the moving boundary, $s(t)$, by deriving some extra conditions there. Differentiating $u(s(t), t) = 0$ with respect to t gives

$$\frac{\mathrm{D}u}{\mathrm{D}t} = \frac{\partial u}{\partial t} + \left.\frac{\partial u}{\partial x}\right|_{x=s} \frac{\mathrm{d}s}{\mathrm{d}t} = 0. \tag{5}$$

Using (1) and (3) this reduces to

$$\frac{\partial^2 u}{\partial x^2} = 1, \quad \text{at} \quad x = s. \tag{6}$$

Also, differentiating $u_x(s(t), t) = 0$ with respect to t gives

$$\frac{\partial^2 u}{\partial x \partial t} + \left.\frac{\partial^2 u}{\partial x^2}\right|_{x=s} \frac{\mathrm{d}s}{\mathrm{d}t} = 0. \tag{7}$$

Now, from (1) we have

$$\frac{\partial^2 u}{\partial x \partial t} = \frac{\partial^3 u}{\partial x^3} \tag{8}$$

and so substituting (6) and (8) into (7) gives

$$\frac{ds}{dt} = -\frac{\partial^3 u}{\partial x^3}, \quad \text{at} \quad x = s, \tag{9}$$

as developed by Crank and Gupta [1]. Conditions (6) and (9) are often used in addition to, or instead of, the other conditions at the moving boundary.

3. Short time solution

As discussed in Crank and Gupta [1], the initial condition (4) shows that in the steady-state a negative unit gradient of concentration exists at the surface. When the surface is sealed a zero surface gradient is instantaneously imposed in accordance with (2). There will be an interval of time, however, before the disturbance at the surface has an effect on the solution in the neighbourhood of $x = 1$. Thus an analytical solution can be obtained for small times, by assuming that the boundary $s = 1$ does not initially move.

The short time problem is therefore

$$\frac{\partial u}{\partial t} = \frac{\partial^2 u}{\partial x^2} - 1, \quad 0 < x < 1, \tag{10}$$

$$\frac{\partial u}{\partial x} = 0, \quad \text{at} \quad x = 0, \tag{11}$$

$$u = 0, \quad \text{at} \quad x = 1, \tag{12}$$

$$u = \frac{1}{2}(1-x)^2, \quad 0 \leqslant x \leqslant 1, \quad \text{at} \quad t = 0, \tag{13}$$

which can be solved exactly using Laplace transforms or separation of variables. The former gives

$$u(x,t) = \frac{1}{2}(1-x)^2 + 2\sqrt{\frac{t}{\pi}}\sum_{n=0}^{\infty}(-1)^n\left[\exp\left\{-\left(\frac{2n+2-x}{2\sqrt{t}}\right)^2\right\} - \exp\left\{-\left(\frac{2n+x}{2\sqrt{t}}\right)^2\right\}\right]$$
$$-\sum_{n=0}^{\infty}(-1)^n\left[(2n+2-x)\operatorname{erfc}\left(\frac{2n+2-x}{2\sqrt{t}}\right) - (2n+x)\operatorname{erfc}\left(\frac{2n+x}{2\sqrt{t}}\right)\right], \tag{14}$$

whilst the latter leads to

$$u(x,t) = \frac{1}{2}(x^2-1) + \sum_{n=0}^{\infty}A_n\cos\left[(n+1/2)\pi x\right]\exp\left[-(n+1/2)^2\pi^2 t\right], \tag{15}$$

where

$$A_n = \frac{8}{\pi^2(4n^2+4n+1)}, \quad n = 0, 1, 2, \ldots. \tag{16}$$

This solution requires seven terms in the sum in order to obtain a solution that does not vary to within 16 decimal places. However, the Laplace transform solution only requires two terms and, in fact, the first term in (14) is a very good approximation. Setting $n = 0$ gives

$$u(x,t) \sim \frac{1}{2}(1-x)^2 + 2\sqrt{\frac{t}{\pi}}\left[\exp\left\{-\left(\frac{2-x}{2\sqrt{t}}\right)^2\right\} - \exp\left\{-\left(\frac{x}{2\sqrt{t}}\right)^2\right\}\right] - \left[(2-x)\operatorname{erfc}\left(\frac{2-x}{2\sqrt{t}}\right) - x\operatorname{erfc}\left(\frac{x}{2\sqrt{t}}\right)\right]. \tag{17}$$

In Fig. 1 we plot the approximation (17) and the numerical solution of (1)–(4) for various small times. We see that the convergence of the infinite series in (14) is very rapid and so terms corresponding to $n = 0$ are sufficient over a small time interval.

4. Integral methods applied to the original system

4.1. The Crank and Gupta method

Crank and Gupta [1] apply an integral method to the system (1)–(4). They claim that integral methods are not very amenable in cases of non-uniform initial distributions and that the discontinuity in the surface gradient is an additional difficulty. In order to apply an integral method they first determine an expression for the surface concentration and use it as an additional boundary condition. From their numerical solution they deduce that the surface concentration can be approximated by the small time solution (17). In fact, they simplify this further and use

$$u(0,t) = \frac{1}{2} - 2\sqrt{\frac{t}{\pi}}. \tag{18}$$

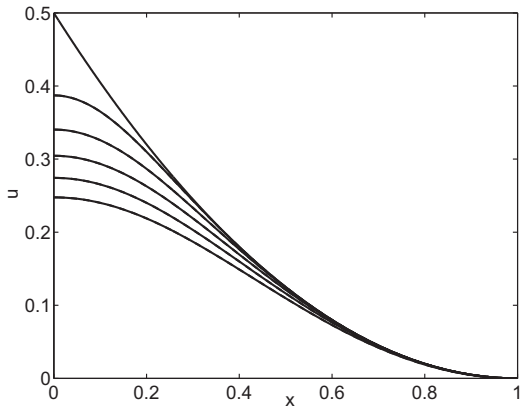

Fig. 1. Concentration distributions for $t = 0, 0.01, 0.02, 0.03, 0.04, 0.05$. The solid line shows the numerical solution of (1)–(4) and the dashed line shows the first term in the series solution, (17).

To satisfy the boundary conditions at $x = s$ they choose a quartic profile centred at $x = s$, i.e.,

$$u = a_2\left(1-\frac{x}{s}\right)^2 + a_3\left(1-\frac{x}{s}\right)^3 + a_4\left(1-\frac{x}{s}\right)^4, \tag{19}$$

which automatically satisfies the conditions in (3). The coefficients a_i are then obtained using the boundary conditions (2), (6) and (18). On writing $u_0(t)$ for $u(0,t)$ the polynomial (19) becomes

$$u = \frac{s^2}{2}\left(1-\frac{x}{s}\right)^2 + (4u_0(t) - s^2)\left(1-\frac{x}{s}\right)^3 - (3u_0(t) - s^2/2)\left(1-\frac{x}{s}\right)^4. \tag{20}$$

The integral method then integrates (1) from $x = 0$ to $x = s$ to obtain

$$\frac{\mathrm{d}}{\mathrm{d}t}\int_0^s u\,\mathrm{d}x = -s, \tag{21}$$

using the fact that $u_x(0,t) = u(s,t) = u_x(s,t) = 0$. Substituting the profile (19) gives an ODE to solve for s, namely

$$\frac{\mathrm{d}s}{\mathrm{d}t} = -\frac{[20 + 8u_0'(t)]s}{8u_0(t) + s^2}. \tag{22}$$

Since $\mathrm{d}s/\mathrm{d}t \leqslant 0$ it follows that $20 + 8u_0'(t) \geqslant 0$. If $u_0(t)$ satisfies (18) then this reduces to

$$t \geqslant \frac{4}{25\pi}. \tag{23}$$

Hence this method can only start at $t = t^*$, with $t^* = 4/[25\pi]$ and $s(t^*) = 1$.

4.2. The Gupta and Banik method

In 1989 Gupta and Banik [28] wrote a technical note describing an alteration to Crank and Gupta's approach. Their method does not rely on imposing a surface concentration in advance, unlike Crank and Gupta who made use of (18). Gupta and Banik specify a quartic polynomial, centred at $x = 0$, which satisfies boundary conditions (2), (3) and (6). It is given by

$$u(x,t) = u_0 + \frac{1}{2}(s^2 - 12u_0)\left(\frac{x}{s}\right)^2 + (8u_0 - s^2)\left(\frac{x}{s}\right)^3 + \frac{1}{2}(s^2 - 6u_0)\left(\frac{x}{s}\right)^4, \tag{24}$$

where again $u_0 = u(0,t)$. Here u_0 and s are determined from combining the integral (21), which they call the *zeroth moment*, with the *first moment*. This is derived from multiplying the PDE by x before integrating from $x = 0$ to $x = s$. After applying integration by parts and using the boundary conditions the integral becomes

$$\frac{\mathrm{d}}{\mathrm{d}t}\int_0^s xu\,\mathrm{d}x = u|_{x=0} - \frac{1}{2}s^2. \tag{25}$$

This is similar to a recent formulation, known as the refined integral method [22,29] where the PDE is integrated twice over the spatial domain. The resulting integral is

$$s\frac{\mathrm{d}}{\mathrm{d}t}\int_0^s u\,\mathrm{d}x - \frac{\mathrm{d}}{\mathrm{d}t}\int_0^s xu\,\mathrm{d}x = -u|_{x=0} - \frac{1}{2}s^2, \tag{26}$$

which does differ from (25), but both expressions are the identical if we eliminate the first integral in (26) using (21). Obviously, when solving both these integrals it does not make any difference whether we solve (21) and (25) or (21) and (26). This method is related to the *combined integral method* (CIM), which has been successfully employed by Mitchell and Myers for thermal and Stefan problems [23,26]. The difference there is that a combination of the zeroth and first moments are used to determine a possibly time dependent unknown exponent along with the moving boundary position. This is discussed in more detail in Section 5.

The resulting ODEs are given by

$$\frac{du_0}{dt} = -\frac{5s^4 + 30s^2u_0 + 240u_0^2}{s^2(5s^2 + 24u_0)}, \quad \frac{ds}{dt} = -\frac{60(s^2 - 4u_0)}{s(5s^2 + 24u_0)}. \tag{27}$$

From the physics of the problem it is clear that $ds/dt \leqslant 0$, and so from the second equation we see that this method requires $s^2 - 4u_0 \geqslant 0$. Since $s(0) = 1$ it follows that $u_0(0) \leqslant 0.25$. This is incompatible with the initial condition at $t = 0$ and so, similar to Crank and Gupta, this method can also only start at time $t = t^* > 0$, with the assumption that $s(t^*) = 1$. One way to determine t^* here is to use (18): solving $u_0 \leqslant 0.25$ gives $t \geqslant \pi/64 \approx 0.0490874$. However, for comparison purposes we use the same value as Crank and Gupta, namely $t^* = 4/[25\pi] \approx 0.050930$, and substituting this into (18) gives $u_0(t^*) = 0.23569 < 0.25$.

Results for the Crank and Gupta and Gupta and Banik profiles are shown in Figs. 2 and 3. Since it is hard to distinguish the different solutions for u, we also present errors in u in Table 1, compared to the numerical solution [9] using the infinity norm. These are analysed further in Section 5.2,, to enable comparisons with the other approximate integral solutions described below.

4.3. Applying an integral method to a transformed problem

Although both the Crank and Gupta and Gupta and Banik profiles are reasonably accurate, they are both very restrictive because they cannot be solved from $t = 0$. More importantly, they require use of the small time solution to either determine $u(0, t)$ or a starting value $u_0(t^*)$. The moving position s does not vary in this interval but the solution for the concentration does (with the position of the left boundary changing from 0.5 at $t = 0$ to ≈0.25 at $t = t^*$ for both methods, see Fig. 1). We now develop a method that can be started from $t = 0$, without any need to combine with the short time solution, and which is more accurate than either of the methods described above.

The methods described above do not make use of the initial condition in (10), and as we have already mentioned, integral methods do not work well when the initial profile is non-uniform. An obvious starting point is therefore to subtract off the initial condition, i.e., by setting

$$v(x, t) = u(x, t) - \frac{1}{2}(1 - x)^2, \tag{28}$$

which means that v satisfies

$$\frac{\partial v}{\partial t} = \frac{\partial^2 v}{\partial x^2}, \quad 0 < x < s, \tag{29}$$

$$\frac{\partial v}{\partial x} = 1, \quad \text{at} \quad x = 0, \tag{30}$$

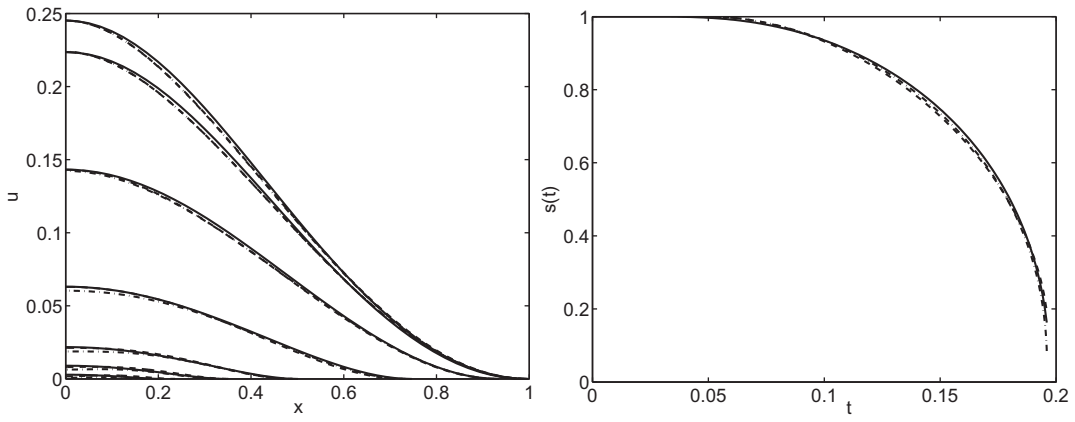

Fig. 2. The left plot shows u against x (at $t = 4/[25\pi]$, 0.06, 0.1, 0.15, 0.18, 0.19, 0.195) and the right plot shows s against t. The solid line is the numerical solution, the dashed line is the Crank and Gupta profile and the dot-dashed line is the Gupta and Banik profile.

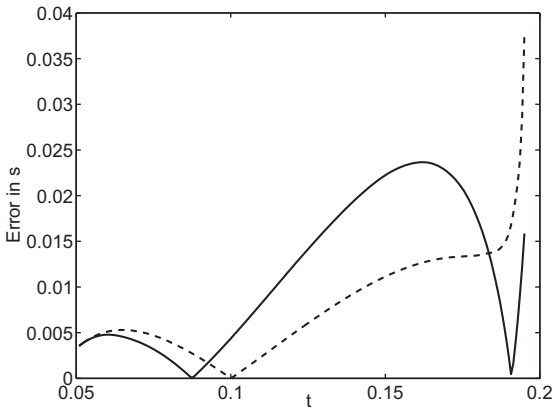

Fig. 3. Plot of the absolute error in s for the Crank and Gupta profile (solid line) and the Gupta and Banik profile (dashed line).

Table 1
Comparison of the infinity norms of u at various times.

Time t	Crank and Gupta (20)	Gupta and Banik (24)
$4/[25\pi]$	3.893×10^{-3}	3.893×10^{-3}
0.060	4.093×10^{-3}	3.999×10^{-3}
0.100	2.227×10^{-3}	2.537×10^{-3}
0.150	4.476×10^{-4}	2.683×10^{-3}
0.180	9.008×10^{-4}	2.950×10^{-3}
0.190	8.663×10^{-4}	2.591×10^{-3}
0.195	1.159×10^{-3}	2.132×10^{-3}

$$v = -\frac{1}{2}(1-s)^2, \quad \text{at} \quad x = s, \tag{31}$$

$$\frac{\partial v}{\partial x} = 1 - s, \quad \text{at} \quad x = s, \tag{32}$$

$$v = 0, \quad \text{at} \quad t = 0. \tag{33}$$

For convenience we write (31) and (32) as

$$v = f(s), \quad \frac{\partial v}{\partial x} = g(s), \quad \text{at} \quad x = s, \tag{34}$$

where $f(s) = -(1-s)^2/2$ and $g(s) = 1 - s$. Since the flux condition at $x = s$ is now non-zero we can use a profile of the form

$$v(x,t) = a_0 + a_1\left(1 - \frac{x}{s}\right) + a_n\left(1 - \frac{x}{s}\right)^n. \tag{35}$$

This form was first used by Myers and Mitchell [25,26] for classic Stefan problems. After satisfying the boundary conditions it becomes

$$v(x,t) = f - gs\left(1 - \frac{x}{s}\right) - \frac{s}{n}(1-g)\left(1 - \frac{x}{s}\right)^n. \tag{36}$$

Here the integral can be written as

$$\frac{\mathrm{d}}{\mathrm{d}t}\int_0^s v\,\mathrm{d}x - f\frac{\mathrm{d}s}{\mathrm{d}t} = g - 1, \tag{37}$$

and substituting the profile v in (36), along with the expressions for $f$and g, leads to the solution

$$s = \left(1 - \frac{4n(n+1)t}{n^2+n-6}\right)^{1/2}. \tag{38}$$

Note that this requires the restriction

$$t < \frac{n^2+n-6}{4n(n+1)}, \tag{39}$$

to ensure that s is real. It also forces $n^2 + n - 6 > 0$ which means that $n > 2$. This condition is very restrictive since, for example, if $n = 3$ then the condition (39) becomes $t < 0.125$ and from Fig. 2 it is clear that s is still close to 1 at $t = 0.125$. Hence this profile leads to very inaccurate solutions.

5. Further transformations

5.1. Analysis of the small time fixed boundary problem

The above analysis shows that it is not enough to simply subtract off the initial condition. Therefore, we now re-examine the small time problem given by (10)–(13) and consider the point $(0, 0)$. Now,

$$\lim_{t\to 0} u(0,t) = \frac{1}{2}, \quad \lim_{x\to 0} u(x,0) = \frac{1}{2}, \tag{40}$$

where the first limit is determined using the exact solution (14), and so u is consistent at $(x, t) = (0, 0)$. The initial condition (13) gives $u_x(x,0) = -(1-x)$ which shows

$$\lim_{t\to 0} u_x(0,t) = 0, \quad \lim_{x\to 0} u_x(x,0) = -1. \tag{41}$$

Hence u_x is inconsistent at $(0, 0)$.

Let us subtract off the initial condition, as done in Section 4.3, by re-writing the system in terms of v (defined in (28)). The problem for v here is then

$$\frac{\partial^2 v}{\partial x^2} = \frac{\partial v}{\partial t}, \quad 0 < x < 1, \tag{42}$$

$$\frac{\partial v}{\partial x} = 1, \quad \text{at} \quad x = 0, \tag{43}$$

$$v = 0, \quad \text{at} \quad x = 1, \tag{44}$$

$$v = 0, \quad \text{at} \quad t = 0. \tag{45}$$

Then

$$\lim_{t\to 0} v(0,t) = 0, \quad \lim_{x\to 0} v(x,0) = 0, \tag{46}$$

$$\lim_{t\to 0} v_x(0,t) = 1, \quad \lim_{x\to 0} v_x(x,0) = 0, \tag{47}$$

and so this does not remove the inconsistency in the derivative.

Suppose we consider the identical problem to (42)–(45) but on a semi-infinite domain i.e.,

$$\frac{\partial^2 \hat{v}}{\partial x^2} = \frac{\partial \hat{v}}{\partial t}, \quad 0 < x < \infty, \tag{48}$$

$$\frac{\partial \hat{v}}{\partial x} = 1, \quad \text{at} \quad x = 0, \tag{49}$$

$$\hat{v} \to 0, \quad \text{at} \quad x \to \infty, \tag{50}$$

$$\hat{v} = 0, \quad \text{at} \quad t = 0. \tag{51}$$

This has exact solution

$$\hat{v}(x,t) = x\,\text{erfc}\left(\frac{x}{2\sqrt{t}}\right) - 2\sqrt{\frac{t}{\pi}}\exp\left(-\frac{x^2}{4t}\right). \tag{52}$$

We now return to the system (42)–(45) and subtract $\hat{v}$ from v by setting

$$w(x,t) = v(x,t) - x\,\text{erfc}\left(\frac{x}{2\sqrt{t}}\right) + 2\sqrt{\frac{t}{\pi}}\exp\left(-\frac{x^2}{4t}\right). \tag{53}$$

Then (42)–(45) transform to

$$\frac{\partial^2 w}{\partial x^2} = \frac{\partial w}{\partial t}, \quad 0 < x < 1, \tag{54}$$

$$\frac{\partial w}{\partial x} = 0, \quad \text{at} \quad x = 0, \tag{55}$$

$$w = -\text{erfc}\left(\frac{1}{2\sqrt{t}}\right) + 2\sqrt{\frac{t}{\pi}}\exp\left(-\frac{1}{4t}\right), \quad \text{at} \quad x = 1, \tag{56}$$

$$w = 0, \quad \text{at} \quad t = 0. \tag{57}$$

Now, from (53) it follows that

$$w_x(x,t) = v_x(x,t) - \text{erfc}\left(\frac{x}{2\sqrt{t}}\right),$$

and so, using this along with (52), (53) and the limits in (46) and (47) we find

$$\lim_{t\to 0} w(0,t) = \lim_{x\to 0} w(x,0) = 0, \quad \lim_{t\to 0} w_x(0,t) = \lim_{x\to 0} w_x(x,0) = 0.$$

The transformation therefore leads to consistency in both w and w_x at $(0, 0)$.

5.2. The moving boundary problem

Following this approach we re-formulate the moving boundary problem (29)–(33) by applying the transformation in (53). Then the problem for w becomes

$$\frac{\partial w}{\partial t} = \frac{\partial^2 w}{\partial x^2}, \quad 0 < x < s, \tag{58}$$

$$\frac{\partial w}{\partial x} = 0, \quad \text{at} \quad x = 0, \tag{59}$$

$$w = -\frac{1}{2}(1-s)^2 - s\,\text{erfc}\left(\frac{s}{2\sqrt{t}}\right) + 2\sqrt{\frac{t}{\pi}}\exp\left(-\frac{s^2}{4t}\right), \quad \text{at} \quad x = s, \tag{60}$$

$$\frac{\partial w}{\partial x} = 1 - s - \text{erfc}\left(\frac{s}{2\sqrt{t}}\right), \quad \text{at} \quad x = s, \tag{61}$$

$$w = 0, \quad \text{at} \quad t = 0. \tag{62}$$

Similar to (34), it is convenient to re-write (60) and (61) as

$$w = f(s,t), \quad s\frac{\partial w}{\partial x} = g(s,t), \quad \text{at} \quad x = s, \tag{63}$$

where

$$f(s,t) = -\frac{1}{2}(1-s)^2 - s\,\text{erfc}\left(\frac{s}{2\sqrt{t}}\right) + 2\sqrt{\frac{t}{\pi}}\exp\left(-\frac{s^2}{4t}\right), \tag{64}$$

$$g(s,t) = s\left[1 - s - \text{erfc}\left(\frac{s}{2\sqrt{t}}\right)\right]. \tag{65}$$

The reason for the inclusion of s in the left hand side of (63)(b) is to give a neater form for the coefficients in the profiles discussed below. Note that the extra condition (6) becomes

$$s^2\frac{\partial^2 w}{\partial x^2} = h(s,t), \quad h(s,t) = \frac{s^2}{\sqrt{\pi t}}\exp\left(-\frac{s^2}{4t}\right), \tag{66}$$

at $x = s$, where again the addition of s^2 turns out to be more convenient.

We begin by defining a cubic polynomial profile of the form

$$w(x,t) = a_0 + a_1\left(1 - \frac{x}{s}\right) + a_2\left(1 - \frac{x}{s}\right)^2 + a_3\left(1 - \frac{x}{s}\right)^3. \tag{67}$$

After satisfying the conditions in (59) and (63), and re-writing a_2 as a, we have

$$w(x,t) = f - g\left(1 - \frac{x}{s}\right) + a\left(1 - \frac{x}{s}\right)^2 - \frac{1}{3}(2a - g)\left(1 - \frac{x}{s}\right)^3. \tag{68}$$

Here a is an unknown coefficient which must be determined along with s. This is similar to u_0 in the Gupta and Banik profile (24) but here a is not the surface concentration. Since $w = 0$ at $t = 0$, in addition to $f = g = 0$, it follows that $a(0) = 0$.

We use the same idea as Gupta and Banik and define the zeroth and first moments. To determine the integral for the zeroth moment we integrate (58) with respect to x over the interval $[0, s]$. This leads to

$$\frac{\mathrm{d}}{\mathrm{d}t}\int_0^s w\,\mathrm{d}x - w|_{x=s}\frac{\mathrm{d}s}{\mathrm{d}t} = \left.\frac{\partial w}{\partial x}\right|_{x=s} - \left.\frac{\partial w}{\partial x}\right|_{x=0}, \tag{69}$$

whilst the first moment becomes (after multiplying by x before integrating)

$$\frac{\mathrm{d}}{\mathrm{d}t}\int_0^s xw\,\mathrm{d}x - sw|_{x=s}\frac{\mathrm{d}s}{\mathrm{d}t} = s\left.\frac{\partial w}{\partial x}\right|_{x=s} - w|_{x=s} + w|_{x=0}. \tag{70}$$

Substituting the profile (68) into both of these expressions gives

$$\frac{\mathrm{d}}{\mathrm{d}t}\left[\frac{s}{12}(2a - 5g + 12f)\right] - f\frac{\mathrm{d}s}{\mathrm{d}t} = \frac{g}{s}, \tag{71}$$

$$\frac{\mathrm{d}}{\mathrm{d}t}\left[\frac{s^2}{20}(a - 3g + 10f)\right] - sf\frac{\mathrm{d}s}{\mathrm{d}t} = \frac{1}{3}(g + a). \tag{72}$$

Noting that

$$\frac{\mathrm{d}f}{\mathrm{d}t} = f_s\frac{\mathrm{d}s}{\mathrm{d}t} + f_t, \quad \frac{\mathrm{d}g}{\mathrm{d}t} = g_s\frac{\mathrm{d}s}{\mathrm{d}t} + g_t, \tag{73}$$

which are all known, Eqs. (71) and (72) can be written as a pair of first order ODEs to solve for a and s.

Following Gupta and Banik, we could use a quartic profile with the extra condition (66). After satisfying (59), (63) and (66) we have

$$w(x,t) = f - g\left(1 - \frac{x}{s}\right) + \frac{h}{2}\left(1 - \frac{x}{s}\right)^2 + b\left(1 - \frac{x}{s}\right)^3 - \frac{1}{4}(3b - g + h)\left(1 - \frac{x}{s}\right)^4. \tag{74}$$

Again it turns out that $b(0) = 0$ and substituting this profile into (69) and (70) gives similar ODEs to (71) and (72).

Alternatively, we can consider a profile with an unspecified exponent, similar to (35). The profile is given by

$$w(x,t) = f - g\left(1 - \frac{x}{s}\right) + \frac{g}{n}\left(1 - \frac{x}{s}\right)^n, \tag{75}$$

where $n \geqslant 1$, and which satisfies the conditions in (59) and (63). Substituting this expression into the integral (69) leads to

$$\frac{\mathrm{d}}{\mathrm{d}t}\left[fs - \frac{(n^2 + n - 2)gs}{2n(n+1)}\right] - f\frac{\mathrm{d}s}{\mathrm{d}t} = \frac{g}{s}. \tag{76}$$

In this case there is only one ODE to solve for s, once a value for n has been specified (without randomly assigning it apriori). One such approach to determine the exponent would be to use the combined integral method (CIM) [23,26]. In a similar manner to that described above, this method combines the zeroth and first moments and so $n \equiv n(t)$ would be solved for, along with s, in the resulting pair of ODEs. However, it is not always easy to calculate $n(0)$, and quite often n is very close to constant for a large range of t.

In Fig. 4 we plot the solution for s and u for three values of n ($= 1.25, 1.5, 2$). It is interesting to note that the accuracy of the solution varies dramatically with n, with the natural choice $n = 2$ being the worst of the three results shown. It seems that the most accurate solution occurs when $n \approx 1.25$. An alternative way to find n is to use the Myers method [24,25] which chooses the value of n to minimise the Langford [30] error

$$E_n = \int_0^s \left[\frac{\partial w}{\partial t} - \frac{\partial^2 w}{\partial x^2}\right]^2 \mathrm{d}x. \tag{77}$$

The resulting expression is time dependent since it involves s, f, g and their derivatives. It addition, E_n has a singularity at $n = 1.5$. For more standard Stefan problems n is typically in the range $[1.7, 3]$ and so this singularity is not a problem. We actually only require $n > 1$ and it seems from Fig. 4 that choosing $n < 1.5$ gives a more accurate solution. In Fig. 5(a) we plot E_n against n at $t = 0$. There is only one local minimum at $n \approx 2.7318$ but this value leads to highly inaccurate results. From examining the plot in Fig. 5, $E_n = 0$ at $n \approx 1.2733$, which agrees with our earlier prediction that n is close to 1.25. It should be noted that Myers use the value of n which minimises the expression for E_n at $t = 0$, since typically this is where the largest error occurred. For this problem the error E_n defined in (77) increases with time and so it might not seem sensible to follow the same approach. However, for larger times E_n is negative for all $n < 1.5$, and so using the error expression at $t = 0$ does seem preferable. Indeed, this is further supported by the plot in Fig. 5(b). It shows the infinity error norm in s (between the approximation found from solving (76) and the numerical solution) for the range $t \in [0, 0.18]$ as a function of n. We see that the error is minimised for approximately the same value of n.

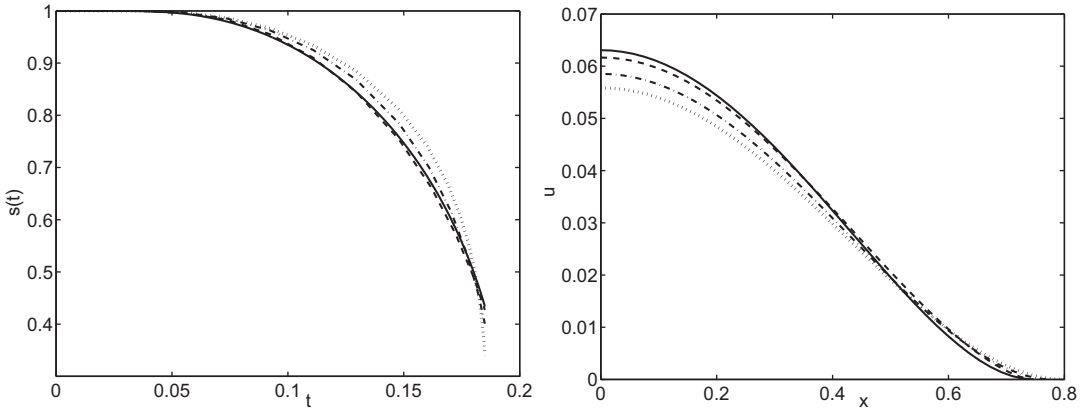

Fig. 4. Solution (74) compared with the numerical solution (solid line) for three values of n (dashed line is $n = 1.25$, dot-dashed line is $n = 1.5$ and dotted line is $n = 2$. The left plot shows s against t and the right plot shows u against x at $t = 0.15$.

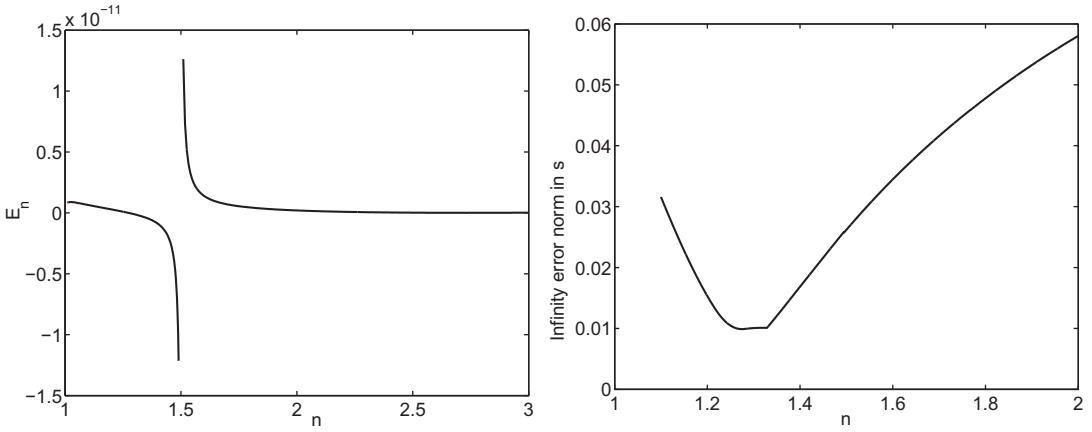

Fig. 5. The left plot shows E_n against n at $t = 0$ and the right plot shows the infinity error norm in s against n.

Finally, note that for all three profiles for w considered in this Section, i.e. (68), (74) and (75), the corresponding profile for u is given by

$$u(x,t) = \frac{1}{2} + x\,\mathrm{erfc}\left(\frac{x}{2\sqrt{t}}\right) - 2\sqrt{\frac{t}{\pi}}\exp\left(-\frac{x^2}{4t}\right) + w(x,t). \tag{78}$$

Figs. 6 and 7 present results of the three profiles along with the numerical solution [9]. In Fig. 6 we show u against x for various times, and the left plot can be directly compared to Fig. 2. All these profiles are more accurate than either the Crank and Gupta or Gupta and Banik profiles, and this is confirmed in the comparison of the infinity norms for the errors in u which are shown in Table 2 (as compared with Table 1). In the right plot in Fig. 6 we show results for u against x for $t < 4/[25\pi]$, to highlight the fact that all the profiles (68), (74) and (75) can be solved from $t = 0$ (computationally when solving the ODEs in Matlab we had to set the minimum time to be $\mathcal{O}(10^{-9})$), unlike the Crank and Gupta or Gupta and Banik profiles. These are all extremely accurate, with no visible distinction from the numerical solution.

In Fig. 7 we plot s against t and the absolute error in s when compared to the numerical solution. On comparison with these and Figs. 2 and 3 it is clear that all the profiles from this Section are more accurate for s than the Crank and Gupta and Gupta and Banik profiles, with the only exception being the limit $t \to t_e^-$ whereby $s(t_e) \to 0$. We discuss this situation in more detail below. On comparing the three profiles (68), (74) and (75) it is difficult to judge which one is preferable. It is clear that there is very little benefit in adding an extra term to give the quartic profile since the results shown in Table 2 are very similar. The non-polynomial profile (75) requires solving only one ODE, rather than the two ODEs (68), (74), but then it does require calculating n using the E_n measure. What is significant is that applying integral methods to the transformed equations leads to much more accurate solutions than previous integral solutions, and allows the process to be started at $t = 0$.

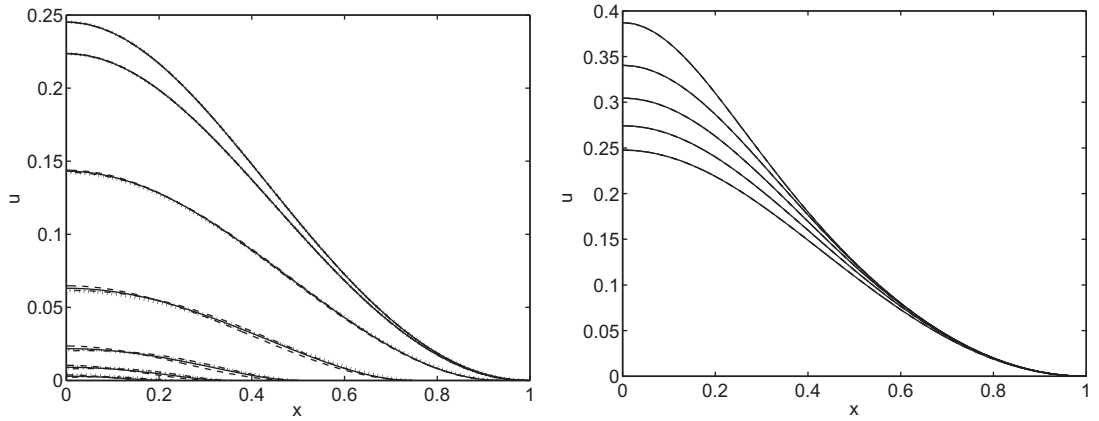

Fig. 6. Plots of u against x. Left is at times $t = 4/[25\pi]$, 0.06, 0.1, 0.15, 0.18, 0.19, 0.195 and right is at $t = 0.01$, 0.02, 0.03, 0.04, 0.05. The solid line is the numerical solution, the dashed line is the cubic profile (68), the dot-dashed line is the quartic profile (74) and the dotted line is profile (75).

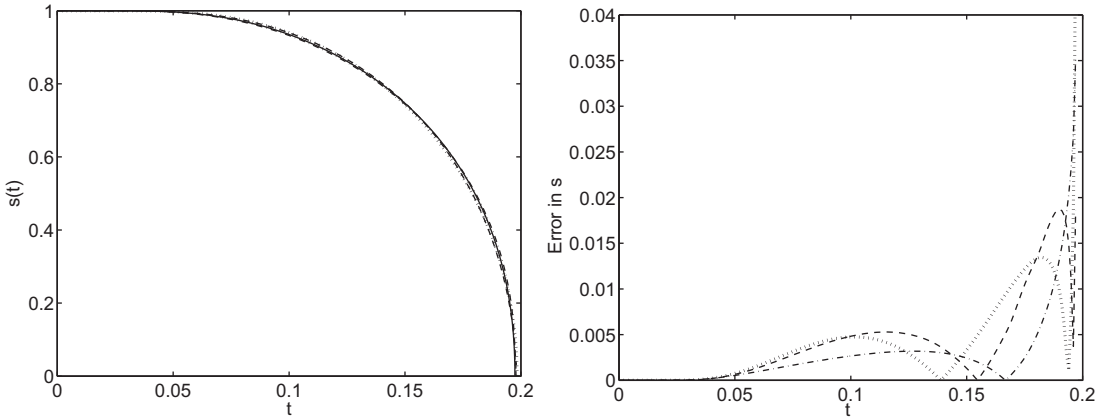

Fig. 7. The left plot shows s against t where the solid line is the numerical solution, the dashed line is the cubic profile (68), the dot-dashed line is the quartic profile (74) and the dotted line is the profile (75). The right plot shows the absolute error in s for these same profiles.

Table 2
Comparison of the infinity norms of u at various times.

Time t	Cubic profile (68)	Quartic profile (74)	Non-polynomial profile (75)
$4/[25\pi]$	1.853×10^{-4}	1.976×10^{-4}	1.705×10^{-4}
0.060	3.612×10^{-4}	3.321×10^{-4}	3.132×10^{-4}
0.100	1.378×10^{-3}	9.609×10^{-4}	1.023×10^{-3}
0.150	1.995×10^{-3}	1.509×10^{-3}	1.979×10^{-3}
0.180	1.785×10^{-3}	1.395×10^{-3}	1.310×10^{-3}
0.190	1.365×10^{-3}	1.069×10^{-3}	8.404×10^{-4}
0.195	9.267×10^{-4}	7.292×10^{-4}	7.551×10^{-4}

Let us now examine the limit $t \to t_e^-$. The numerical solution from [9] predicts $t_e = 0.19743241$. To determine approximate values using the five profiles considered here we solve the ODEs on the interval $[0, t^*]$ and check the sign of s and $\mathrm{d}s/\mathrm{d}t$. Provided both $s > 0$ and $\mathrm{d}s/\mathrm{d}t < 0$ are satisfied, the value of t^* is updated to $t^* = t^* + 10^{-8}$ and the process repeated until either of the criteria fails. Results are shown in Table 3. It is important to give the values of s at t_e, denoted s_e, as well as the errors in t_e when compared with the numerical value of t_e. Whilst profiles (20) and (74) both have the smallest errors, $\mathcal{O}(10^{-5})$, the value of s_e is large. This is because the ODEs have failed due to $\mathrm{d}s/\mathrm{d}t$ becoming positive. Profiles (68) and (75) are therefore far more acceptable because the ODEs allow s to become much closer to zero whilst also predicting a very accurate value of t_e. It should be noted that Crank and Gupta approximate t_e by setting the surface concentration approximation (18)

Table 3
Comparison of the profiles as $t \to t_e$.

Profile	t_e	s_e	Absolute error in t_e
Crank and Gupta profile (20)	0.19750	0.1127	6.764×10^{-5}
Gupta and Banik profile (24)	0.19608	0.04434	1.355×10^{-3}
Cubic profile (68)	0.19787	1.4584×10^{-4}	4.379×10^{-4}
Quartic profile (74)	0.19740	0.04545	3.037×10^{-5}
Non-polynomial profile (75)	0.19837	3.379×10^{-4}	9.341×10^{-4}

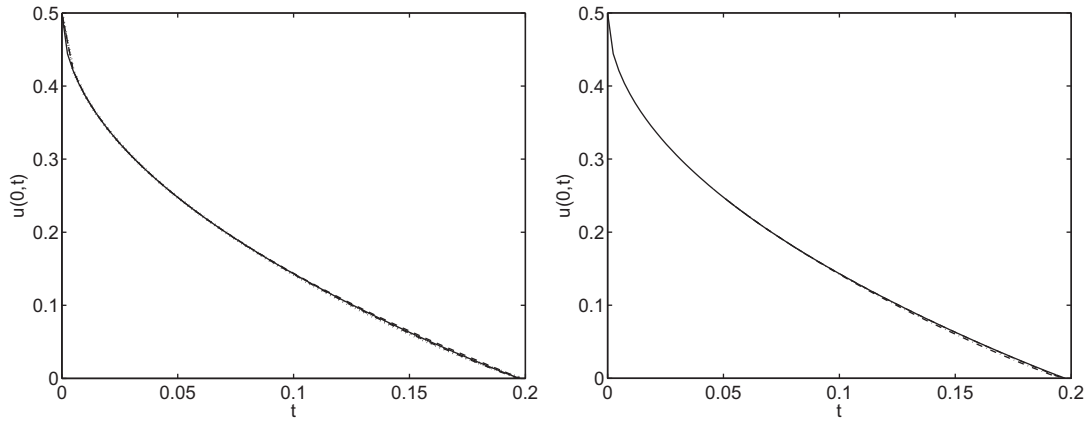

Fig. 8. $u(0,t)$ against t (solid line is the numerical solution): In the left plot the dashed line is the cubic profile (68), the dot-dashed line is the quartic profile (74) and the dotted line is the profile (75). In the right plot the dashed line is the Crank and Gupta profile whilst the dot-dashed line is the Gupta and Banik profile.

to zero. This gives $t_e = \pi/16 \approx 0.19635$ which has error 1.083×10^{-3}. In Fig. 8 we present results comparing $u(0,t)$ against t for the various profiles. The left plot shows the same profiles as discussed in Figs. 6 and 7 and the right plot shows the Crank and Gupta and Gupta and Banik profiles. All methods are good at predicting the evolution of the fixed boundary; the Crank and Gupta profile. appears to be slightly more accurate but this is misleading since it uses the extra boundary condition (18) which is derived from the short time solution.

6. Conclusions

In this study we have considered a variety of integral methods applied to the classic moving boundary problem that arises from the diffusion of oxygen in absorbing tissue. We began by giving the short time solution and then described the Crank and Gupta [1] and Gupta and Banik [28] profiles which made use of this solution since their approach could not be solved from $t = 0$. An analysis of the short time problem at $(x, t) = (0, 0)$ led to a transformation which removed any inconsistencies and this was then applied to the original problem. Two polynomial profiles were considered for this transformed system which were analogous to the cubic and quartic profiles favoured by Crank and Gupta and Gupta and Banik that were discussed in Section 4. In addition, we also described an optimal profile which incorporated an unknown exponent to be determined as part of the solution process. The results for these three profiles were very similar, but all more accurate than those described in Section 4. Crucially, they could all be solved from $t = 0$ and the ODEs gave a better prediction of the time to depletion which also enabled s to become closer to zero.

It is interesting that both the quartic profiles (24) and (74) were overall the least accurate overall. It might be expected that using an extra term in the polynomial would lead to more accurate results, as has been seen in the classic Stefan problem [22], but this was not the case here. These higher order polynomials came from using the boundary conditions (6) and (9), which involve higher order derivatives in x, and so we conclude that these extra conditions not beneficial for oxygen diffusion problems. Indeed, the profile (75) gave more accurate results and only involves three terms, with the value of n close to 1. It is hard to argue whether profile (68) or (75) is more preferable, but the latter does have marginally smaller errors when examining Table 2, and also requires solving only one ODE to determine s.

Whilst one could argue that the oxygen diffusion problem is rather limited in scope, it has been extensively studied in the literature in the past forty years. Despite this, we have demonstrated that up until now there are still unresolved issues related to the integral solutions, and we have addressed these in this paper. An interesting future direction would be to investigate applying these types of transformations to other moving boundary problems with non-uniform initial distributions to develop accurate integral solutions for more general situations.

References

[1] J. Crank, R.S. Gupta, A moving boundary problem arising from the diffusion of oxygen in absorbing tissue, J. Inst. Math. Appl. 10 (1972) 19–33.
[2] S.G. Ahmed, An approximate method for oxygen diffusion in a sphere with simultaneous absorption, Int. J. Numer. Methods Heat Fluid Flow 9 (6) (1999) 631–642.
[3] S.G. Ahmed, A numerical method for oxygen diffusion and absorption in a sike cell, Appl. Math. Comput. 173 (2006) 668–682.
[4] S. Catal, Numerical approximation for the oxygen diffusion problem, Appl. Math. Comput. 145 (2003) 361–369.
[5] V. Gulkac, Comparative study between two numerical methods for oxygen diffusion problem, Commun. Numer. Methods Eng. 25 (2009) 855–863.
[6] R.S. Gupta, N.C. Banik, Constrained integral method for solving moving boundary problems, Comput. Methods Appl. Mech. Eng. 67 (1988) 211–221.
[7] R.S. Gupta, A. Kumar, Complete numerical solution of the oxygen diffusion problem involving a moving boundary, Comput. Methods Appl. Mech. Eng. 29 (1981) 233–239.
[8] R.S. Gupta, A. Kumar, Variable time step method with coordinate transformation, Comput. Methods Appl. Mech. Eng. 44 (1984) 91–103.
[9] S.L. Mitchell, M. Vynnycky. The oxygen diffusion problem: analysis and numerical solution, Int. J. Numer. Methods Fluids (2013), submitted for publication.
[10] S.L. Mitchell, M. Vynnycky, Finite-difference methods with increased accuracy and correct initialization for one-dimensional Stefan problems, Appl. Math. Comput. 215 (2009) 1609–1621.
[11] S.L. Mitchell, M. Vynnycky, An accurate finite-difference method for ablation-type Stefan problems, J. Appl. Comput. Math. 236 (2012) 4181–4192.
[12] S.L. Mitchell, M. Vynnycky, I.G. Gusev, S.S. Sazhin, An accurate numerical solution for the transient heating of an evaporating droplet, Appl. Math. Comput. 217 (2011) 9219–9233.
[13] T.R. Goodman, The heat-balance integral and its application to problems involving a change of phase, Trans. ASME 80 (1958) 335–342.
[14] T.R. Goodman, Application of integral methods to transient nonlinear heat transfer, Adv. Heat Trans. 1 (1964) 51–122.
[15] T.R. Goodman, J.J. Shea, The melting of finite slabs, J. Appl. Mech. 27 (1960) 16–27.
[16] K. Pohlhausen, Zur naherungsweisen Integration der Differentialgleichunger der laminaren Grenzschicht, J. Appl. Math. Mech. ZAMM 1 (1921) 252–290.
[17] H. Schlichting, Boundary Layer Theory, eighth ed., Springer, 2000.
[18] S.L. Mitchell, An accurate nodal heat balance method with spatial subdivision, Numer. Heat Trans. B 60 (2011) 34–56.
[19] S.L. Mitchell, Applying the combined integral method to one-dimensional ablation, Appl. Math. Comput. 36 (2012) 127–138.
[20] S.L. Mitchell, T.G. Myers, Approximate solution methods for one-dimensional solidification from an incoming fluid, Appl. Math. Comput. 202 (1) (2008) 311–326.
[21] S.L. Mitchell, T.G. Myers, A heat balance integral method for one-dimensional finite ablation, AIAA J. Thermophys. 22 (3) (2008) 508–514.
[22] S.L. Mitchell, T.G. Myers, Application of standard and refined heat balance integral methods to one-dimensional Stefan problems, SIAM Rev. 52 (1) (2010) 57–86.
[23] S.L. Mitchell, T.G. Myers, Improving the accuracy of heat balance integral methods applied to thermal problems with time dependent boundary conditions, Int. J. Heat Mass Transfer 53 (2010) 3540–3551.
[24] T.G. Myers, Optimizing the exponent in the heat balance and refined integral methods, Int. Commun. Heat Mass Transfer 36 (2) (2009) 143–147.
[25] T.G. Myers, Optimal exponent heat balance and refined integral methods applied to Stefan problems, Int. J. Heat Mass Transfer 53 (2010) 1119–1127.
[26] T.G. Myers, S.L. Mitchell, Application of the combined integral method to stefan problems, Appl. Math. Model. 35 (2011) 4281–4294.
[27] T.G. Myers, S.L. Mitchell, G. Muchatibaya, M.Y. Myers, A cubic heat balance integral method for one-dimensional melting of a finite thickness layer, Int. J. Heat Mass Transfer 50 (2007) 5305–5317.
[28] R.S. Gupta, N.C. Banik, Approximate method for the oxygen diffusion problem, Int. J. Heat Mass Transfer 32 (1989) 781–783.
[29] N. Sadoun, E-K. Si-Ahmed, P. Colinet, On the refined integral method for the one-phase Stefan problem with time-dependent boundary conditions, Appl. Math. Model. 30 (2006) 531–544.
[30] D. Langford, The heat balance integral method, Int. J. Heat Mass Transfer 16 (1973) 2424–2428.